

# CONCEPTS FOR VELOCITY AND ACCELERATION ESTIMATION EMPLOYING NONUNIFORM SAMPLING

L. Benner<sup>\*\*\*</sup>, W. Wilkening<sup>\*\*</sup> and H. Ermert<sup>\*\*\*</sup>

<sup>\*</sup>Institute of High Frequency Engineering, Faculty of Electrical Engineering,  
 Ruhr-Universität Bochum, Germany

<sup>\*\*</sup>Ruhr Center of Excellence for Medical Engineering, Bochum, Germany

<sup>\*\*\*</sup>TomTec Imaging Systems, Unterschleissheim, Germany

Lars@Benner-net.de

**Abstract:** Our group has previously proposed non-uniform sampling for flow velocity estimation. Standard Pulsed Wave Doppler (PWD) systems acquire an ensemble of  $N$  echoes per beam line at a constant pulse repetition frequency  $f_{prf}$ . The total time span determines the velocity resolution, and  $f_{prf}$  the unambiguous velocity range. The ensemble size  $N$  is by approximation inversely proportional to the frame rate, assuming that the system performs interleaving. If sampling the intervals are chosen nonuniformly, the total time span can be increased, while keeping  $N$  and the shortest sampling interval constant. In this example, velocity range and frame rate are unchanged, and measurement accuracy for low flow velocities is gained at the expense of measurement accuracy of high flow velocities. The extended time span makes the flow estimation susceptible to effects of acceleration and decorrelation. Thus, we have refined the flow estimation algorithms by taking into account both effects. Also the results are compared to standard velocity estimation algorithm.

## Introduction

Conventional PW Doppler systems acquire an ensemble of  $N$  echoes per beam at a constant repetition interval  $T_{pri} = 1/f_{prf}$ . Nonuniform sampling uses variable intervals lengths. The shortest interval defines the velocity range and longer intervals increase the total time span and, therefore, the velocity resolution without increasing  $N$  (With interleaving, the frame rate is approximately reciprocal to  $N$ ). Thus, relative velocity resolution for low velocities is gained the expense of relative velocity resolution at high velocities and SNR. This concept, which is known from RADAR [2,4], has previously been adapted to medical ultrasound by our group, where cross correlation techniques are applied to all pairs of echoes (not only to consecutive echoes) in the ensemble to determine scatter displacement [5].

Two problems still had to be tackled: With increasing time span, acceleration becomes relevant. This effect has to be considered to avoid ambiguity and incorrect velocity estimations. High flow velocities cause decorrelation. To measure slow axial flow velocities, it is important to exclude pairs of echoes that decorrelated due to lateral or elevational flow.

## Pulse Sequence

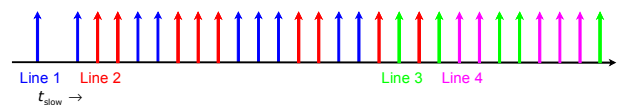


Figure 1: The proposed sequence is interleaving compatible. Spaces longer than  $1T_{pri}$  can be filled with acquisitions for other beam lines. Note that the sequences for line 2, 4 etc. are time reversed.

The nonuniform pulse sequence discussed here is designed to have pulse intervals of different length distributed evenly over the total time span, where all length are multiples of the shortest interval  $T_{pri}$ . Furthermore, it is interleaving compatible, i.e. all intervals longer than  $T_{pri}$  can be used to acquire echoes for other beam lines.

## Modified Cross Correlation

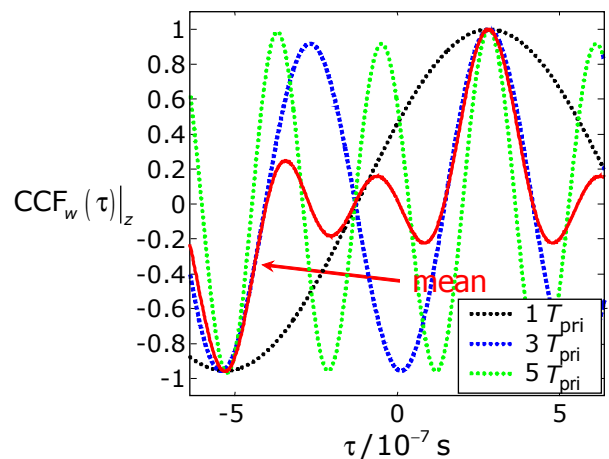


Figure 2: CCFs calculated from simulated data. They are normalized to the energies within the sliding windows and rescaled so that the time lag  $\tau$  is proportional to the velocity independent of the time interval. The CCF for the shortest time interval ( $1T_{pri}$ ) exhibits only one maximum, i.e. it is aliasing free. The CCFs for longer intervals show ambiguities, but the maxima are narrower, i.e. a better velocity resolution can be achieved. Taking the mean of the CCFs trades velocity resolution for unambiguity.

To estimate the flow velocity at a given depth  $z$ , all pairs of echo signals, i.e. not only pair of echoes, are analyzed with respect to time shifts caused by moving

scatterers. For a pair of echoes, the modified cross correlation functions (CCF) considers data within two sliding windows in either of the two echoes, where the windows are positioned symmetrically to the depth  $z$ . The time lag  $\tau$ , being the distance between the centers of the windows in axial or fast time direction, for which the CCF is maximal, is considered to be proportional to the axial displacement of scatterers. To avoid false maxima, which occur, if one window contains signals from a strong scatterer, the CCF values are normalized to the signal energies within the two windows. The CCFs will represent different time intervals. For a given velocity  $v$ , the displacement and, therefore, the time lag  $\tau$  is proportional to the time interval. We rescale the CCF to the time interval so that  $\tau$  is proportional to  $v$ . As can be seen in Figure 2, long time intervals lead to narrower maxima, i.e. better velocity resolution, while shorter intervals have less or no ambiguities (fewer maxima).

### Velocity and Acceleration Estimation

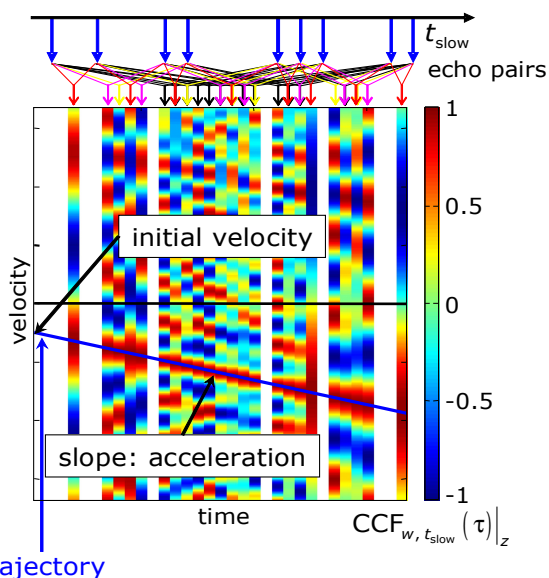


Figure 3: V-T diagram showing cross correlation functions (see Figure 2) along the slow time axis. Some pairs of echo signals may be centered on the same point of the slow time axis. In such cases, the functions are averaged.

The CCFs as illustrated in Figure 2 represent a point on the slow time axis (see Figure 1) that is defined by the center of the time interval. To account for acceleration, we arrange the CCFs along the slow time axis. The resulting diagram will be referred to as a V-T-diagram (V-T-D), see Fig. 3. A trajectory in this diagram describes the velocity as a function of slow time, where a horizontal line corresponds to a constant velocity. The task is to find a trajectory that fits the V-T-diagram best. In the following, different strategies will be presented and analyzed. The strategies are limited by a constant accelerations.

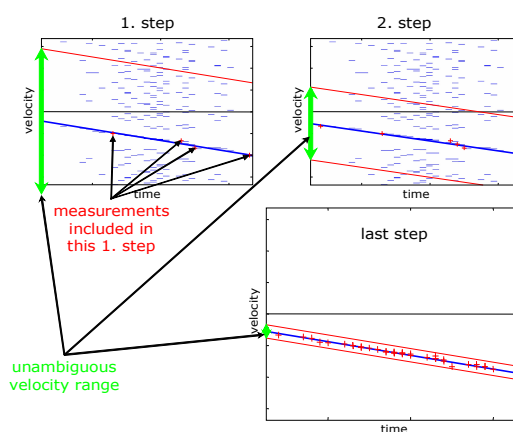


Figure 4: In an iterative process, the initial flow estimate is determined by fitting a line through the maxima of the CCFs corresponding to time intervals of  $IT_{pri}$ . The following steps include longer time intervals. Based on the previous estimates, the search range (red lines) is narrowed to exclude maxima that might be due to aliasing.

### Linear Regression through Maxima of V-T-D

The first approach (Linear Regression through Maxima of V-T-D, LRM) is based on a V-T-D that shows only the maxima of the CCFs, see Figure 4. The trajectory is determined in an iterative process: The first step considers the maxima belonging to the shortest time intervals ( $IT_{pri}$ ). A linear regression through the maxima yields an initial, unambiguous estimate for the trajectory. The next step additionally includes the maxima for an interval length of  $2T_{pri}$ . These CCFs will exhibit additional maxima that are due to aliasing (Figure 2). To exclude those maxima, the search range is narrowed with increasing interval length (Figure 4). The final iteration step includes all interval length. The iteration may also be terminated earlier, if no further maxima are found in the current search range.

### Global Maximum

A second approach is to determine the trajectory along which the sum of CCD values is maximal. The trajectory in Figure 3 fulfills this requirement. It is obvious, however, that the aforementioned sum as a function of velocity and acceleration will be characterized by many local maxima. Thus, the full range of velocities and accelerations is searched in a small enough grid, which is determined by the longest time interval. Once the global maximum is found, the estimate can be refined using gradient-based methods.

### Symmetry Criterion

Figure 3 reveals that the CCFs are symmetrical to the likeliest trajectory. Based on this observation, a third estimator was developed. The optimization criterion is the symmetry of the cross correlation values to a given trajectory. The search method is the same as for the Global Maximum approach.

### Decorrelation and Confidence

We have to differentiate between two sources of decorrelation: One source is given by e.g. motion artifacts, noise, or other kinds of interference. Another source is related to the flow. Elevational and lateral flow components cause decorrelation. Even if flow is purely axial, displacement estimations may not be reliable, unless the displacement is small enough. We therefore, limit the search range for displacements to  $\pm\lambda/4$ . Furthermore, maxima can be excluded (LRM method) or CCF values ignored, if the CCF values are below some threshold. e.g. 0.85.

In addition to velocity and acceleration, a confidence parameter is computed. For all estimation approaches, it is given by the mean of the CCF values along the estimated trajectory, where all values are excluded that are below a certain threshold (0.85) or definitely due to aliasing according to the estimated velocity and the length of the time interval. This confidence value turned out to be a reliable marker of flow.

### Data Acquisition

Data was acquired using a Siemens Sonoline® Antares System equipped with a VF10-5 transducer (linear array, width: 4 cm, center frequency 7.5 MHz). 18 echoes were acquired per beam line at  $f_{prf} = 1099\text{Hz}$ . 9 of the echoes were taken out of the echoes 1-18 representing the proposed pulse sequence. We imaged a flow phantom with a single tube. The tube had a diameter of 10 mm and a slope angle of 25°. RF data was acquired with 16 bits resolution at 40 MHz sampling rate using the Axius Direct Ultrasound Research Interface. To improve the the quality of the measurement, the beams were steered at an angle of 30° so that the angle between the flow direction was 35° degrees. In the following, we will present the data in a rectangle rather than a trapezoid, i.e. the image data is sheared. The shown velocity is the velocity component in sound propagation direction.

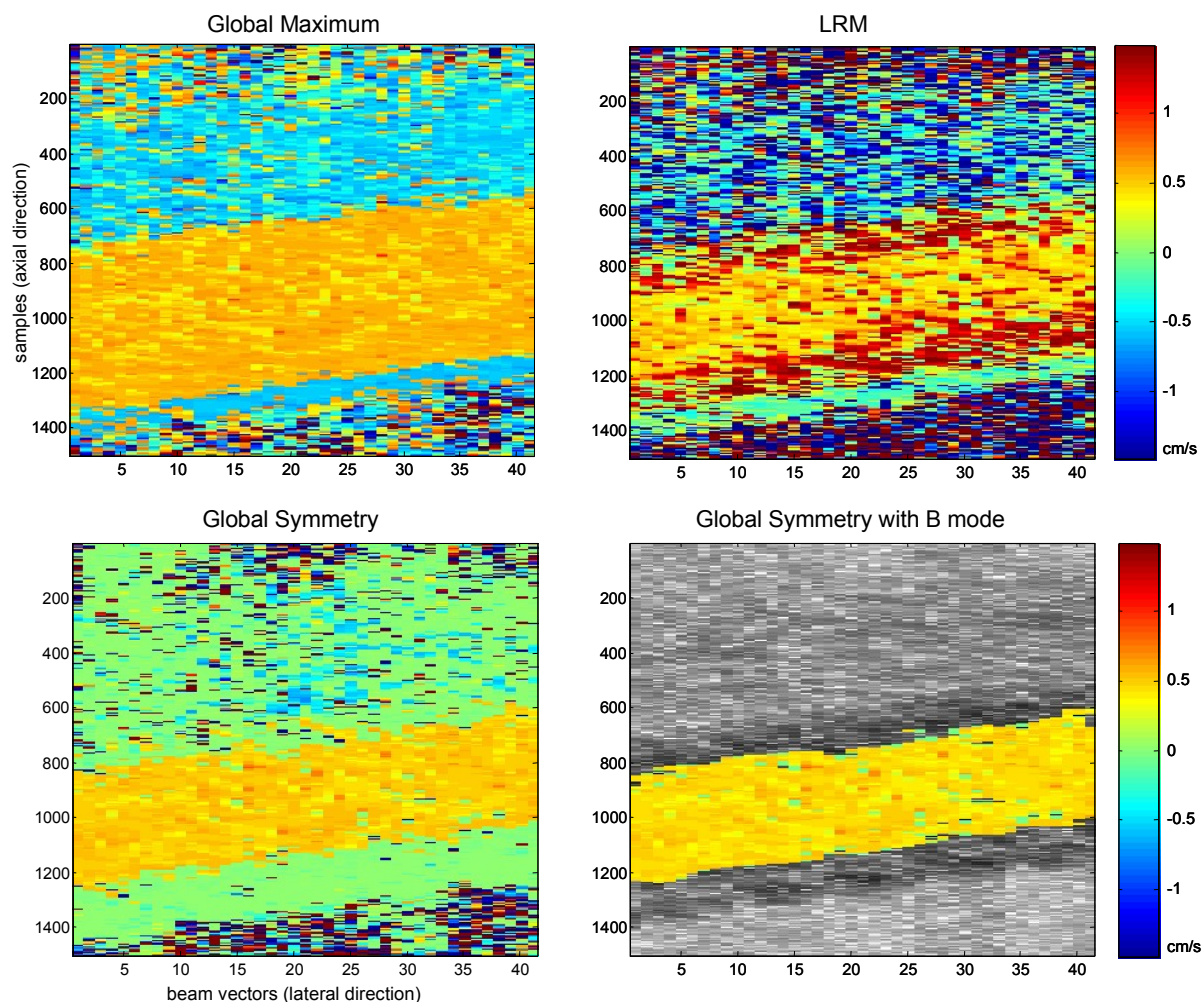


Figure 5: With only 9 echoes per beam line, the proposed nonuniform sampling approach provides satisfactory velocity resolution for low flow at  $f_{prf} = 1099\text{Hz}$ . Especially the Global Symmetry images shows that the velocity estimates are also correct in non flow regions. Global Symmetry with B mode shows the flow estimates combined with a narrow band B mode image calculated from the same echoes as the flow images. The flow decision was performed by thresholding the described confidence parameter.

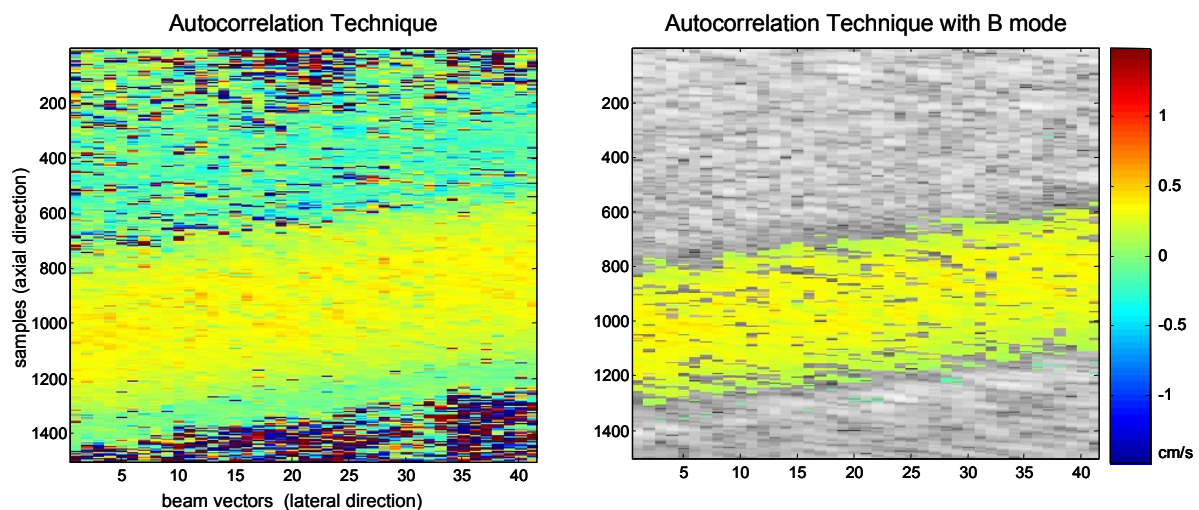


Figure 6: Flow estimation based on an autocorrelation technique. The right image was computed directly with a URI Offline Processing Tool. Unlike to the other images for the computation was a different wallfilter (Eigenvalue-based filter) and additionally clutter rejection used. For the left image the URI algorithm was modified in a way, that only the first 9 beams of an ensemble were used for the calculation and the same wallfilter (DC cancellation) as for the other algorithms was used.

### Autocorrelation as Comparison Method

For an evaluation the calculation results are compared to flow estimations based on an autocorrelation technique [4]. The algorithms were provided by the URI Offline Processing Tools [6].

The previously described properties concerning the resolution, velocity range and frame rate are also valid for this technique valid as well. Therefore, the velocity estimations were also calculated with an ensemble size of  $N=9$ . Since the data was acquired with an ensemble size of  $N=18$ , two simple ways for reducing it are possible: (a) using the first 9 vector of the ensemble (Keeps the shortest interval and the number of echoes the same as for the nonlinear sequence.) or (b) using every second vector of the ensemble (Uses the same total time span, but the shortest time interval is twice as long, i.e. the velocity range is decreased by a factor of 2.).

### Results

The RF data was analyzed by applying the three different algorithms described above. Figure 5 shows the in vitro images for the three different approaches. The LRM algorithm turned out to be the fastest approach, and less robust with respect to noise, while the Symmetry Criterion is the slowest, but the most robust. Hence, it correctly shows the velocity profile that is expected in rigid tubes for slow flow [1].

The results of the nonuniform approach are comparable to the one of the autocorrelation technique, shown in Figure 6, as the difference between the velocities within the tube of around 0,1 cm/s shows.

Acceleration was not taken into account, because the phantom setup had a constant flow, which was confirmed by the calculations.

### Conclusion

These new algorithms yield similar results, where the fastest algorithm (LRM) is the most sensitive to noise and artifacts. The comparison to an autocorrelation approach shows that the results are quite similar. A real advantage of the new approaches are currently not noticeable with constant flow, since neither the wider velocity range nor the ability to measure acceleration could be demonstrated here.

Eventually, real nonuniform sequences have to be implemented, since reverberation may create artifacts that cannot be noticed, if the nonuniform sequence is extracted from a uniform sequence. Also the acceleration estimation has still to be evaluated.

### Acknowledgment

We thank Siemens Medical Systems, Inc., Ultrasound Group for their assistance with the Axis Direct Ultrasound Research Interface.

The work was carried out by the Ruhr Center of Excellence for Medical Engineering (KMR Bochum), BMBF (Federal Ministry of Education and Research, Germany) grant 13N8017.

### References

- [1] JENSEN, J. A. (1996): 'Estimation of blood velocities using ultrasound: a signal processing approach', (Cambridge University Press)
- [2] BENJANIN Z., ZRNIC D. S.(1991): 'Clutter rejection for Doppler weather radars which use staggered pulses', IEEE Transactions on Geoscience and Remote Sensing, vol 29(4), pp. 610-620

- [3] KASAI C., NAMEKAWA K., KOZANO A., OMOTO R. (1985): 'Real-Time Two-Dimensional Blood Flow Imaging Using an Autocorrelation Technique', IEEE Transactions on Sonics and Ultrasonics, VOL. SU-32, NO. 3, may 1985.
- [4] CHOROBOAY E. S., WEBER M. E.(1994): 'Variable-PRI processing for meteorologic Doppler radars', Proceedings of the 1994 IEEE National Radar Conference (1994), pp. 85-90
- [5] WILKENING W., BRENDEL B., ERMERT H. (2002): 'Fast, extended velocity range flow imaging based on nonuniform sampling using adaptive wall filtering and cross correlation.' Proceedings of the IEEE Ultrasonics Symposium, 2002, 2B-3
- [6] The URI Users Group Website:  
<http://www.bme.ucdavis.edu/URI>